Electronic Supplementary Information

Room-Temperature Crystallization of Hybrid-Perovskite Thin Films *via* Solvent-Solvent Extraction for High-Performance Solar Cells

Yuanyuan Zhou, Mengjin Yang, Wenwen Wu, Alexander L. Vasiliev,
Kai Zhu *, and Nitin P. Padture *

* Email: kai.zhu@nrel.gov; nitin_padture@brown.edu

Supplementary Figures:

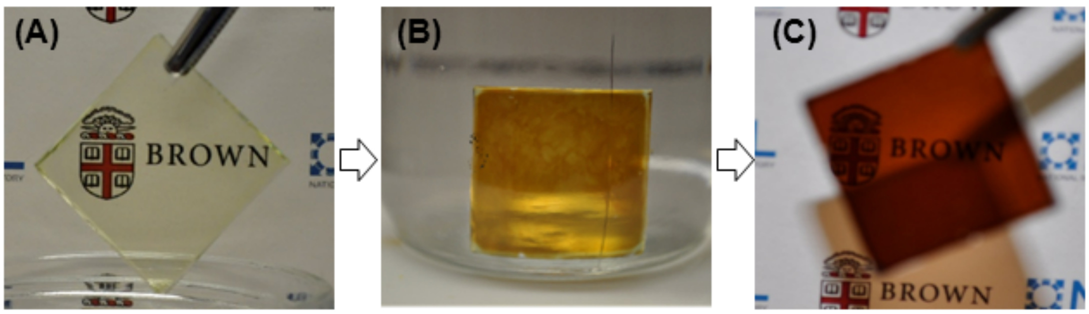

Fig. S1. Photographs of the SSE process in DEE bath: (A) as-spin-coated $MAPbI_3$ precursor thin film, (B) during SSE (2 s), and (C) after SSE (2 min).

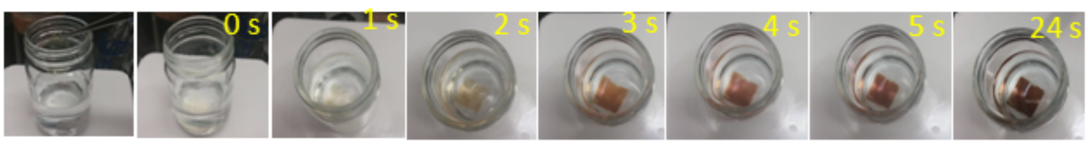

Fig. S2. Sequence of photographs after dropping a spin-coated $MAPbI_3$ precursor thin film (patterned) in DEE bath showing rapid $MAPbI_3$ perovskite thin film formation.

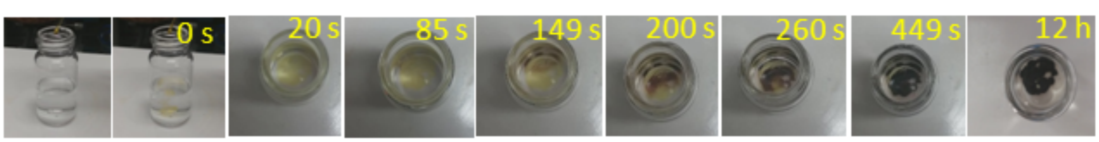

Fig. S3. Sequence of photographs after adding drops of $MAPbI_3$ precursor solution (in NMP) in DEE bath showing sluggish $MAPbI_3$ perovskite precipitate formation.

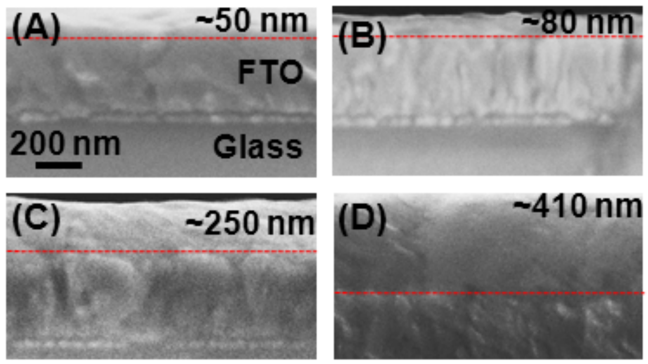

Fig. S4. Cross-sectional SEM images of $MAPbI_3$ perovskite films of various thicknesses deposited on TiO_2-blocking-layer coated FTO-glass substrates using the SSE process at room temperature: (A) ~50 nm, (B) ~80 nm, (C) ~250 nm, and (D) ~410 nm.

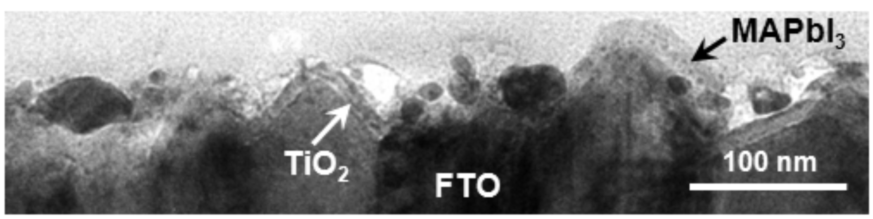

Fig. S5. Cross-sectional bright-field TEM image of a ~20-nm $MAPbI_3$ perovskite film deposited on TiO_2-blocking-layer coated FTO-glass substrate.

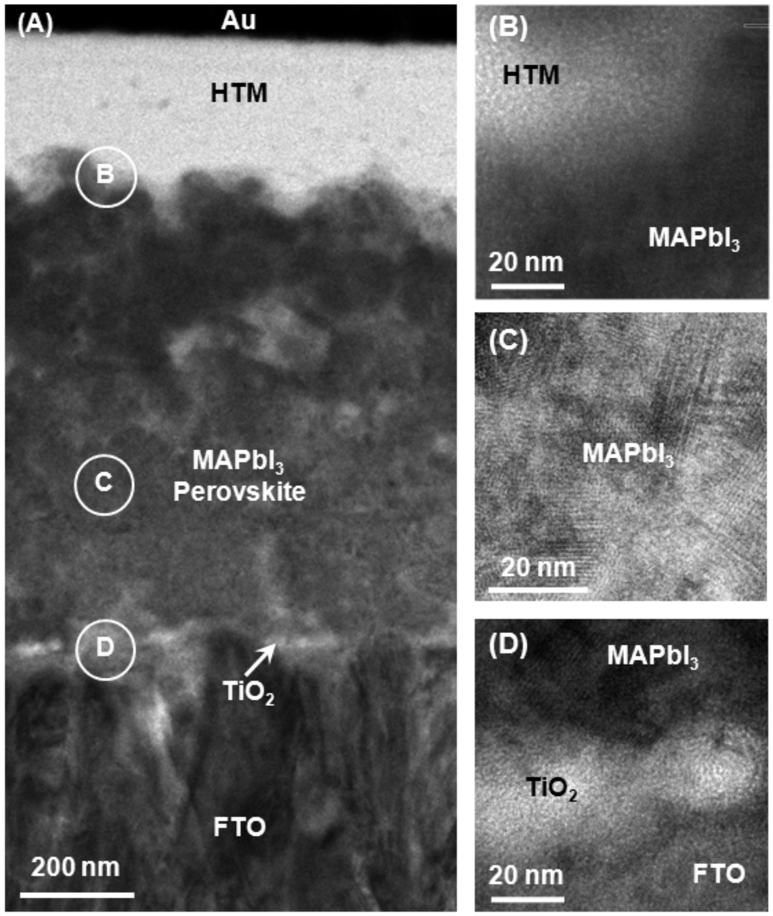

Fig. S6. Bright field TEM images of a typical $MAPbI_3$ perovskite-based solar cell, where the $MAPBI_3$ thin film (~700 nm thickness) is deposited using the SSE process at room temperature: (A) overall view, (B) detailed view of region 'B' showing hole-transporting material (HTM) and $MAPbI_3$, (C) detailed view of region 'C' showing $MAPbI_3$ grains, and (D) detailed view of region 'D' showing $MAPbI_3$, TiO_2 blocking layer and FTO. The thickness of the $MAPbI_3$ layer in this solar cell is unusually thick, and Au was used as the top contact instead of the Ag used in the other cells.

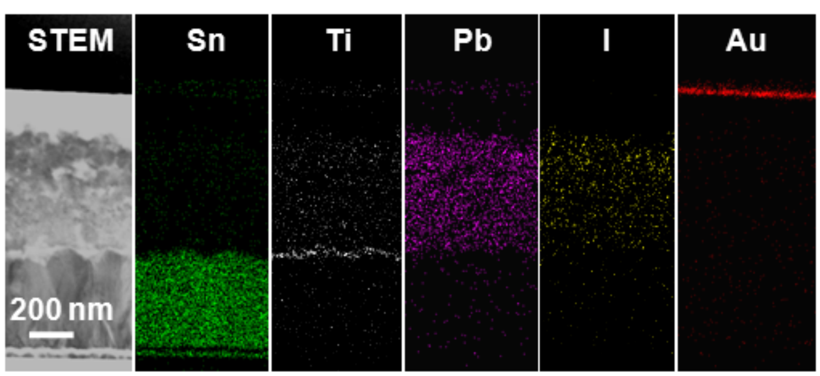

Fig. S7. Elemental EDS mapping of the solar cell in Fig. S6 showing the distribution of elements Sn, Ti, Pb, I, and Au.

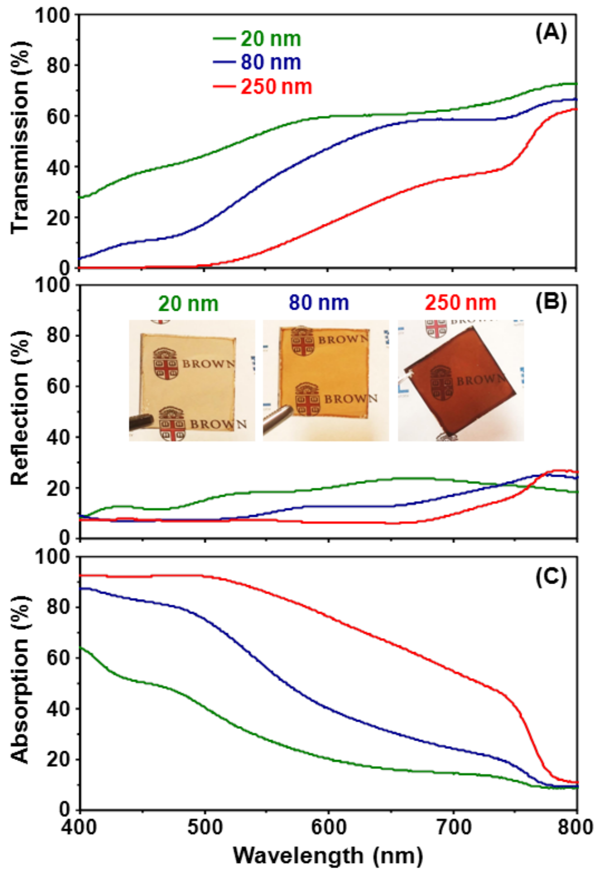

Fig. S8. Optical properties of $MAPbI_3$ perovskite films of various thicknesses deposited on TiO_2-blocking-layer coated FTO-glass substrates using the SSE process at room temperature: (A) transmission, (B) reflection, and (C) absorption. Inset in (B) are photographs of the films.

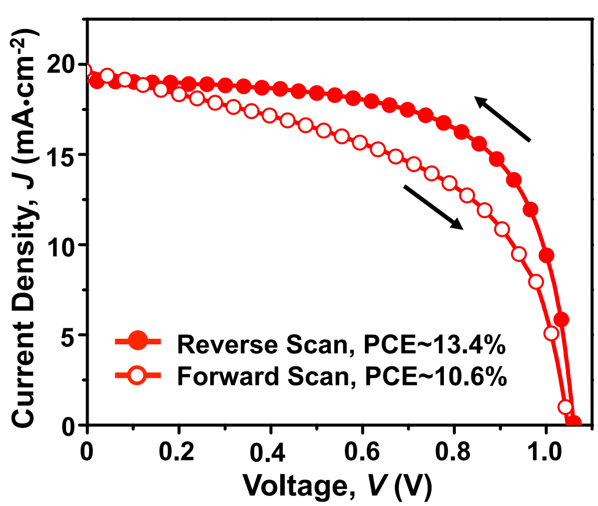

Fig. S9. *J*-*V* characteristics of a PSC based on 250-nm SSE $MAPbI_3$ perovskite thin film, under simulated one-sun AM 1.5G (100 mW cm^{-2}) illumination, in forward (normal) and reverse scan.

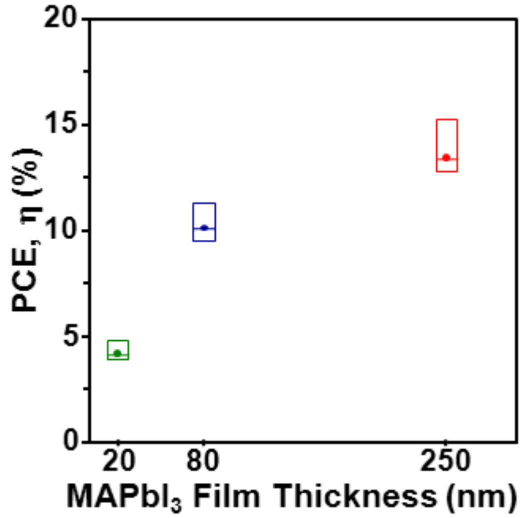

Fig. S10. Mean, minimum and maximum PCE values of PSCs tested under simulated one-sun AM 1.5G (100 mW cm^{-2}) illumination (0.16 cm^2 typical active area) as a function of SSE $MAPbI_3$ perovskite film thickness. About 10-20 solar cells were tested for each thickness.

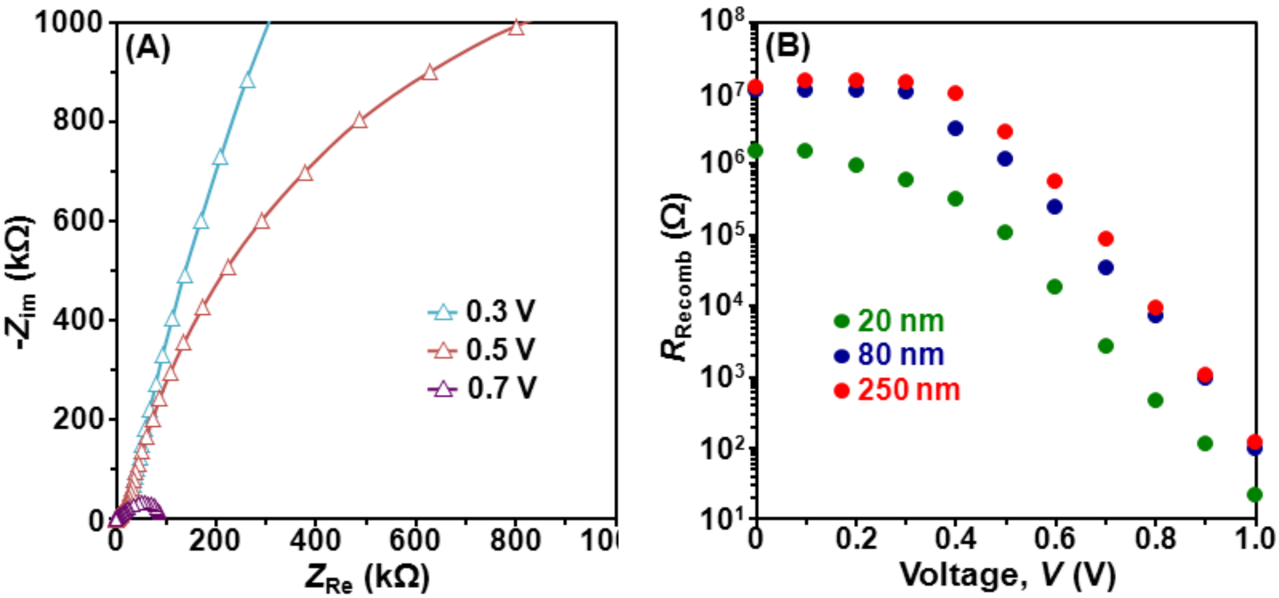

Fig. S11. (A) Typical Nyquist plots of the impedance responses for a solar cell made from SSE $MAPbI_3$ film of ~250 nm thickness, with three different bias voltages. The impedance spectra are dominated by a large semicircle at low frequencies. (B) Plots of recombination resistance as a function of voltage for solar cells with different thickness SSE $MAPbI_3$ perovskite films.

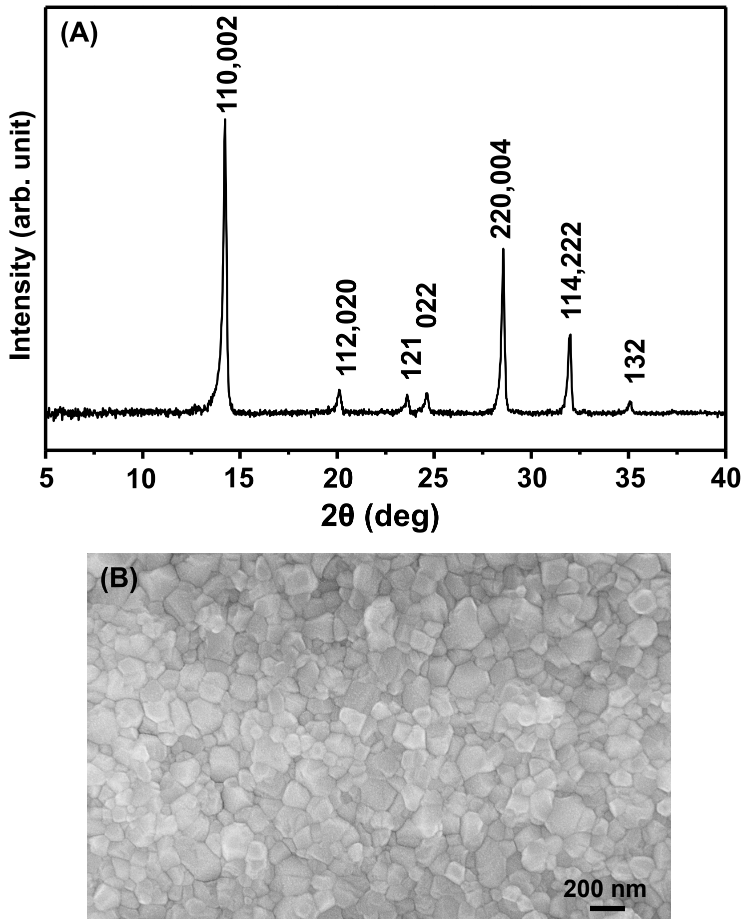

Fig. S12. (A) XRD pattern and (B) SEM micrograph of top surface of 250-nm SSE $MAPbI_3$ perovskite thin film that has been heat-treated at 100 ˚C for 15 min in air.

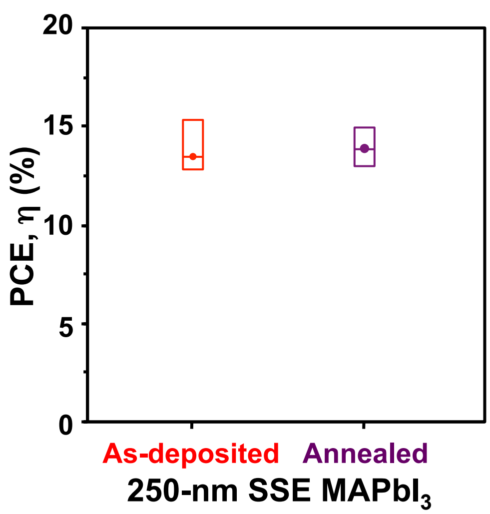

Fig. S13. Mean, minimum and maximum PCE values of PSCs tested under simulated one-sun AM 1.5G (100 mW cm^{-2}) illumination (0.16 cm^2 typical active area) as a function of annealing heat-treatment (100 ˚C, 15 min, in air) of SSE $MAPbI_3$ perovskite films (~250 nm thickness). About 10-20 solar cells each were tested.